Journal of Inclusion Phenomena and Macrocyclic Chemistry (2024) 104:257–268
https://doi.org/10.1007/s10847-024-01228-2

ORIGINAL ARTICLE

Trans-to-cis isomerization of a platinum(II) complex with two triphosphine ligands via coordination with gold(I) ions

Kazuki Nagasato[1] · Taichi Baba[1] · Hayato Soma[2] · Nobuto Yoshinari[1]

Received: 31 January 2024 / Accepted: 27 February 2024 / Published online: 10 May 2024
© The Author(s) 2024

Abstract

The reaction of a square-planar platinum(II) complex containing two bis(2-diphenylphosphinoethyl)phenylphosphine (triphos), $[Pt(triphos)_2](NO_3)_2$, with $[Au(tu)_2]Cl$ (tu = thiourea) gave a new trinuclear $Au^I_2Pt^{II}$ complex, $[Pt(triphos)_2\{Au(tu)\}_2]Cl_2(NO_3)_2$, through Au-P coordination. While the $[Pt(triphos)_2]^{2+}$ unit in $[Pt(triphos)_2](NO_3)_2$ adopted the trans-meso configuration, only the cis-racemic isomer was observed for $[Pt(triphos)_2\{Au(tu)\}_2]Cl_2(NO_3)_2$. ^{31}P NMR spectroscopy indicated rapid equilibrium among the possible isomers of $[Pt(triphos)_2]^{2+}$, which facilitated the trans-to-cis transformation at the Pt^{II} center in this system. Additionally, we observed that this structural transformation led to an increase in the emission intensity.

Keywords Gold(I) ion · Isomerism · Luminescence · Platinum(II) ion · Triphosphine

Introduction

Square-planar platinum(II) complexes are kinetically inert, which often enables the formation of geometric isomers, namely, cis/trans or E/Z isomers [1]. These isomers play crucial roles in influencing the biological activity [2], optical/electronic properties [3], and chemical reactivity [4, 5]. Consequently, controlled syntheses of specific isomers are needed to develop functional platinum(II) coordination compounds. Structural manipulations of platinum(II) complexes, especially those with phosphine ligands, have garnered increasing interest from coordination chemists. This interest is primarily due to the fascinating isomerization behavior and photoluminescent features of these complexes [6]. In 1970, Mastin and Haake reported that a square-planar platinum(II) complex with two triphenylphosphines and two chloride ligands, $[Pt(PPh_3)_2Cl_2]$, showed cis-trans equilibrium in solution and was directed to the trans-isomer by irradiation with UV light [7]. After this report, cis-trans isomerism of platinum(II) complexes with monophosphine or diphosphine ligands was widely studied and utilized for stimuli-responsive systems, such as molecular gears and anion receptors [8–11]. Typically, these compounds featured a platinum(II) center surrounded by two phosphine groups and two heteroatoms, as in $[Pt^{II}(P)_2(X)_2]$. This category of compounds exhibited distinct electronic states, with the total energies differing for the cis and trans isomers [12]. This variability facilitates preferential formation of one isomer or enables isomerization with chemical/physical stimuli. When modified asymmetrically by substituent groups (i.e., $[Pt^{II}(P_A)_2(P_B)_2]$), platinum(II) complexes bound by four phosphine groups can also form cis-trans isomers [13, 14]. These isomers tend to have nearly equal energy levels for the cis and trans isomers, so it is more challenging to regulate isomerism. While several studies have reported crystallization of these isomers [15–18], structural control of the geometric isomers through chemical reactions remains elusive.

In this context, we investigated the stereochemistry of a square-planar platinum(II) complex, $[Pt(triphos)_2]^{2+}$ (triphos = bis(2-diphenylphosphinoethyl)phenylphosphine). This complex was prepared and isolated as an organotin(IV) chloride salt by García-Fernández and coworkers in 2001, who proposed based on ^{31}P and ^{195}Pt NMR spectroscopic results that two of the three phosphorous (P) atoms were bound to Pt^{II} and one terminal P atom remained uncoordinated [19]. Although both cis and trans isomers are theoretically possible for the structure of $[Pt(triphos)_2]^{2+}$, its stereostructure has remained ambiguous due to the absence of crystallographic data. In this study, we crystallized the

✉ Nobuto Yoshinari
nobuto@chem.sci.osaka-u.ac.jp

[1] Department of Chemistry, Graduate School of Science, Osaka University, Toyanaka, Osaka 560- 0043, Japan

[2] Department of Chemistry, School of Science, Osaka University, Toyanaka, Osaka 560-0043, Japan

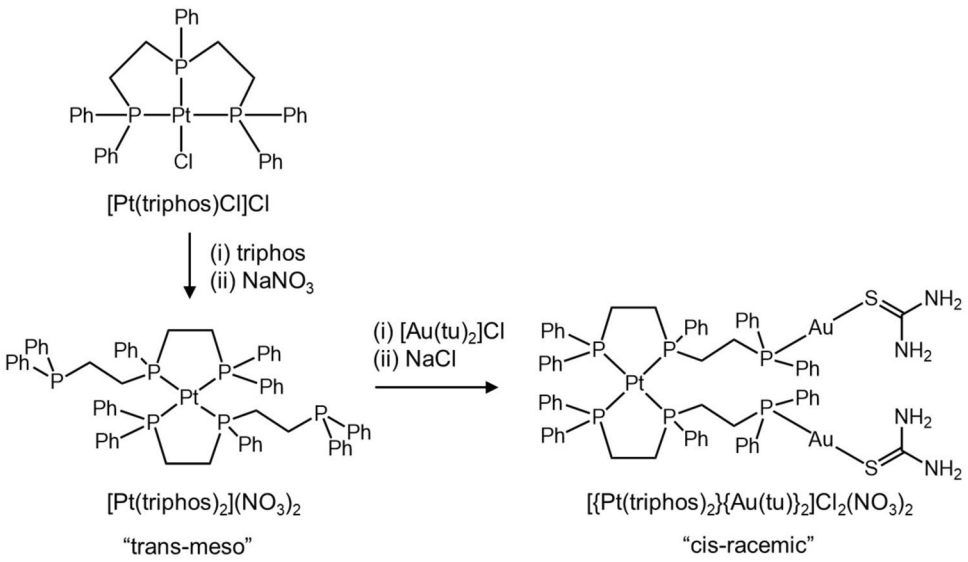

Scheme 1 Synthetic routes to $[Pt(triphos)_2](NO_3)_2$ and $[Pt(triphos)_2\{Au(tu)\}_2]Cl_2(NO_3)_2$

nitrate salt $[Pt(triphos)_2](NO_3)_2$ and determined the structure. X-ray crystallography revealed that the complex $[Pt(triphos)_2](NO_3)_2$ formed the trans isomer, with two uncoordinated phosphorous atoms oriented on opposite sides. Furthermore, the reaction of $[Pt(triphos)_2](NO_3)_2$ with the gold(I) complex $[Au(tu)_2]Cl$ (tu = thiourea) resulted in the formation of a heterometallic $Pt^{II}Au^{I}_2$ complex, $[Pt(triphos)_2\{Au(tu)\}_2]Cl_2(NO_3)_2$. In this complex, the two uncoordinated P atoms in $[Pt(triphos)_2]^{2+}$ were bound by $\{Au^{I}(tu)\}^{+}$ units through Au–P bonds (Scheme 1). This meant that $[Pt(triphos)_2](NO_3)_2$ functioned as a ditopic P-donating metalloligand [20–23]. Notably, while the initial $[Pt(triphos)_2](NO_3)_2$ adopted the trans isomer, the $[Pt(triphos)_2]^{2+}$ unit observed in $[Pt(triphos)_2\{Au(tu)\}_2]^{4+}$ adopted the cis configuration. To our knowledge, trans-to-cis isomerization of a square-planar $[Pt^{II}(P_A)_2(P_B)_2]$ unit via coordination with metal ions is unprecedented. An increase in the photoluminescence was also observed after the transformation from $[Pt(triphos)_2]^{2+}$ to $[Pt(triphos)_2\{Au(tu)\}_2]^{4+}$. The present study demonstrated that combining square-planar Pt^{II} complexes with two linear triphosphine ligands produced a structurally flexible ditopic P-donating metalloligand. Furthermore, the spectroscopic and structural data for the two complexes provide an essential dataset for understanding the cis/trans isomers of $[Pt^{II}(P_A)_2(P_B)_2]$-type square-planar complexes.

Experimental section

Materials

The starting complexes [Pt(triphos)Cl]Cl [24] and $[Au(tu)_2]Cl$ [25] were prepared according to methods described in the literature. Other chemicals were purchased and used without further purification.

Preparation of the complexes

$[Pt(triphos)_2](NO_3)_2{\cdot}CH_2Cl_2$

To a colorless solution containing [Pt(triphos)Cl]Cl (81 mg, 0.10 mmol) in 30 mL of methanol was added 54 mg (0.099 mmol) of triphos and 30 mL of methanol, which yielded a yellow suspension. After stirring for 2 h, 1.0 mL of a 1 M $NaNO_3$ aqueous solution and 15 mL of water were added to the resulting clear yellow solution, which was then slowly evaporated for 3 days. The crude $[Pt(triphos)_2](NO_3)_2$ was collected by filtration and washed with water. The crude product was purified by recrystallization from CH_2Cl_2-*n*-hexane. Yield: 86 mg (58%). Anal. calcd. for $[Pt(triphos)_2](NO_3)_2{\bullet}CH_2Cl_2 = C_{69}H_{68}Cl_2N_2O_6P_6Pt$: C, 56.26; H, 4.65; N, 1.90%. Found: C, 56.45; H, 4.94; N, 2.01%. IR spectrum (cm^{-1}, ATR): 1433, 745 (ν_{P-CH2-}), 1101, 696 (ν_{P-Ph}), 1333 (ν_{NO3^-}). ^1H NMR spectrum (methanol-d_4, 500 MHz), δ: 7.64–6.82 (50 H, m), 2.56–2.16 (15 H, m). $^{31}P\{^1H\}$ NMR spectrum (methanol-d_4, 202 MHz), δ: 45.2 (t, $^1J_{P-Pt} = 1085$ Hz) and 17.9 (t, $^1J_{P-Pt} = 624$ Hz).

$[Pt(triphos)_2\{Au(Tu)\}_2]Cl_2(NO_3)_2{\cdot}5H_2O$

To a solution containing $[Pt(triphos)_2](NO_3)_2{\cdot}CH_2Cl_2$ (51 mg, 0.036 mmol) in 3 mL of methanol was added a solution containing $[Au(tu)_2]Cl$ (31 mg, 0.081 mmol) in 2 mL of methanol. After stirring for 1.5 h at room temperature in the dark, 0.150 mL of an aqueous solution of 1 M NaCl was added to the resulting colorless solution, and Et_2O was diffused in for 7 days. The resulting colorless needle-like

crystals were collected by filtration. Yield: 25 mg (33%). Anal. Calcd. for $[Pt(triphos)_2\{Au(tu)\}_2]Cl_2(NO_3)_2 \bullet 5H_2O = C_{70}H_{84}Au_2Cl_2N_6O_{11}P_6PtS_2$: C, 40.13; H, 4.04; N, 4.01%. Found: C, 40.21; H, 3.88; N, 4.33%. IR spectrum (cm^{-1}, ATR): 3052 (ν_{N-H}), 1435, 753 (ν_{P-CH2-}), 1103, 694 (ν_{P-Ph}), 1330 (ν_{NO3}^-), 1635 ($\nu_{C=S}$). ^1H NMR spectrum (methanol-d_4, 500 MHz), δ: 7.91–6.63 (50 H, m), 3.63–3.37 (3 H, m), 3.17n2.58 (11 H, m). $^{31}P\{^1H\}$ NMR spectrum (methanol-d_4, 202 MHz), δ: 92.2 (t. $^1J_{P-Pt} = 1342$ Hz), 43.4 (t, $^1J_{P-Pt} = 1221$ Hz), 34.6 (s), 33.2 (s).

Physical measurements

IR spectra were recorded with a JASCO FT/IR-4100 infrared spectrophotometer using the ATR method at room temperature. Elemental analyses (C, H, N) were performed at Osaka University with a YANACO CHN Corder MT-5. X-ray fluorescence spectrometry was performed with a SHIMADZU EDX-7000 spectrometer. The TG and DTA measurements were performed with a SHIMADZU DTG-60 system. The PXRD patterns were recorded with a BRUKER D2 PHASER diffractometer at room temperature. ^1H and ^{31}P NMR spectra were recorded with a JEOL ECS400 (400 MHz) spectrometer in methanol-d_4 with tetramethylsilane (TMS) as an internal standard for ^1H spectra and triphenylphosphine as an external standard for ^{31}P spectra. Powder X-ray diffraction (PXRD) measurements were performed under ambient conditions with a BRUKER D2 PHASR diffractometer. The simulated powder patterns were generated from the single-crystal X-ray structures with Mercury 2023.2 [26]. The diffuse solid-state reflection spectra were measured with a JASCO V-670 UV/VIS spectrometer at room temperature using $MgSO_4$. The photoluminescence spectra were recorded with a JASCO FP-8500 spectrometer. The internal emission quantum yields (Φ) were obtained via absolute measurements with an integrating sphere (JASCO ILFC-847); the internal surface was coated with highly reflective Spectralon. An ESC-842 calibrated light source (WI) and an ESC-843 calibrated light source (D2) were used to calibrate the emission intensities and measure the absolute quantum yields.

X-ray structural determinations

The single-crystal X-ray diffraction dataset for $[Pt(triphos)_2](NO_3)_2 \cdot CH_2Cl_2$ was collected at 100 K with a Synergy Custom X-ray diffractometer equipped with a Hypix-6000HE hybrid photon counting detector and a Rigaku VariMax rotating-anode X-ray source with a Mo target (λ = 0.71073 Å). The dataset for $[Pt(triphos)_2\{Au(tu)\}_2]Cl_2(NO_3)_2$ was collected with a PILATUS3 X CdTe 1 M detector with a synchrotron X-ray source at the BL02B1 beamline at Spring-8. The intensity data were collected via the ω-scan technique and empirically corrected for absorption. All structures were solved by the intrinsic phasing method within the SHELXT program [27] and were refined on F^2 by the full-matrix least-squares technique using the SHELXL program [28] via the Olex2 interface [29]. The hydrogen atoms, with the exception of those on the water molecules, were calculated and placed with riding models. All nonhydrogen atoms were refined anisotropically, while the H atoms were refined isotropically. Nitrate anions and water molecules could not be modeled and were, therefore, removed from the electron density map with the Olex2 solvent mask command [29]. ISOR instructions were applied for C35 in $[Pt(triphos)_2](NO_3)_2 \cdot CH_2Cl_2$ and C35 and N2 in $[Pt(triphos)_2\{Au(tu)\}_2]Cl_2(NO_3)_2$.

The crystallographic data are summarized in Table 1. Selected bond distances and angles are summarized in Tables 2 and 3.

Results and discussion

Synthesis and structural characterization of $[Pt(triphos)_2](NO_3)_2$

The reaction of [Pt(triphos)Cl]Cl with one equivalent of triphos in methanol triggered a color change from colorless to yellow. Subsequently, an excess of $NaNO_3$ was added to isolate the nitrate salt of $[Pt(triphos)_2]^{2+}$ as a crude powder. Slow diffusion of *n*-hexane into a solution of the crude powder in CH_2Cl_2 yielded colorless block crystals ($[Pt(triphos)_2](NO_3)_2$) in moderate yield (58%). The IR spectrum of $[Pt(triphos)_2](NO_3)_2$ exhibited an intense band at 1343 cm^{-1} attributed to the ν_{N-O} stretch of the NO_3^- ion, along with sharp signals corresponding to ν_{P-Ph} (1103, 694 cm^{-1}) and ν_{P-C} (1435, 753 cm^{-1}) vibrations of the triphos ligands (Fig. 1a) [30]. The CHN elemental and fluorescence X-ray analyses were consistent with the CH_2Cl_2 adduct $[Pt(triphos)_2](NO_3)_2 \cdot CH_2Cl_2$ (Fig. S1). Thermogravimetric (TG) analyses indicated a weight loss of 3.0% at 92 °C, corresponding to loss of the CH_2Cl_2 molecule of solvation (Fig. S2). This value, which was lower than the theoretical value of 5.6% for the loss of one CH_2Cl_2, suggested the efflorescent nature of $[Pt(triphos)_2](NO_3)_2$.

A single-crystal X-ray analysis of $[Pt(triphos)_2](NO_3)_2$ revealed that the asymmetric unit comprised half of a mononuclear platinum(II) complex cation with two triphos ligands, $[Pt(triphos)_2]^{2+}$, situated at the crystallographic inversion center, and half of a solvated CH_2Cl_2 molecule. Although the NO_3^- ions could not be modeled, they were presumed to occupy the crystal void spaces and were disordered. As illustrated in Fig. 2, each triphos ligand was bonded to the square-planar Pt^{II} center in a bidentate-*P*,*P′* fashion, engaging one of the two terminal PPh_2 groups

Table 1 Crystallographic data for $[Pt(triphos)_2](NO_3)_2{\cdot}CH_2Cl_2$ and $[Pt(triphos)_2\{Au(tu)\}_2]Cl_2(NO_3)_2$

	$[Pt(triphos)_2](NO_3)_2{\cdot}CH_2Cl_2$	$[Pt(triphos)_2\{Au(tu)\}_2]Cl_2(NO_3)_2$
Empirical formula	$C_{69}H_{68}Cl_2P_6Pt$	$C_{70}H_{74}Au_2Cl_2N_4P_6PtS_2$
Formula weight	1349.1	1881.3
Crystal size, mm	0.40 x 0.10 x 0.02	0.08 x 0.04 x 0.01
Crystal system	Triclinic	Monoclinic
Space group	*P*-1	*C*2/*c*
a, Å	10.0577(4)	17.0638(17)
b, Å	10.8441(5)	29.412(3)
c, Å	16.5828(7)	18.0970(18)
α, °	79.317(4)	90
β, °	75.396(4)	90.118(6)
γ, °	79.633(4)	90
V, Å^3	1702.90(13)	9082.4(16)
Z	1	4
T, K	100(2)	100(2)
R (int)	0.0532	0.1333
ρ_{calcd}, g cm^{-3}	1.315	1.376
m (Mo Kα), mm^{-1}	2.317	1.229
θ_{max}	30.7730	15.602
Total no. of data	23129	66104
No. of unique data	8439	10410
No. of parameters	358	393
No. of restraints	6	12
$R1$[a)] $[I>2\sigma(I)]$	0.0443	0.0969
R_w[b)] [All data]	0.0968	0.2057
Largest diff. peak and hole, e.Å^{-3}	2.18 and − 1.68	2.84 and − 1.90

a) $R_1 = \Sigma||F_o| - |F_c||/\Sigma|F_o|$

b) $wR_2 = \{\Sigma w(|F_o| - |F_c|)^2/\Sigma wF_o^2\}^{1/2}$, $w = 1/2\Sigma(F_o)$

Table 2 Selected bond distances and angles for $[Pt(triphos)_2](NO_3)_2{\cdot}CH_2Cl_2$

Bond distances (Å)			
Pt(1)-P(2)	2.3268(9)	Pt(1)-P(3)	2.3190(9)
Angles (°)			
P(3)-Pt(1)-P(3$^{\#1}$)	180.0	P(2)-Pt(1)-P(2$^{\#1}$)	180.0
P(2)-Pt(1)-P(3)	84.04(3)	P(2)-Pt(1)- P(3$^{\#1}$)	95.96(3)

#1: −x,1−y,1−z

Table 3 Selected bond distances and angles for $[Pt(triphos)_2\{Au(tu)\}_2]Cl_2(NO_3)_2$

Bond distances (Å)			
Pt(1)-P(2)	2.311(3)	Au(1)-P(1)	2.265(4)
Pt(1)-P(3)	2.316(3)	Au(1)-S(1)	2.314(5)
Angles (°)			
P(2)-Pt(1)-P(2$^{\#1}$)	95.72(1	P(2)-Pt(1)-P(3$^{\#1}$)	174.12(11)
P(2)-Pt(1)-P(3)	84.51(11)	P(1)-Au(1)-S(1)	174.07(15)

#1: 1−x,+y,1/2−z

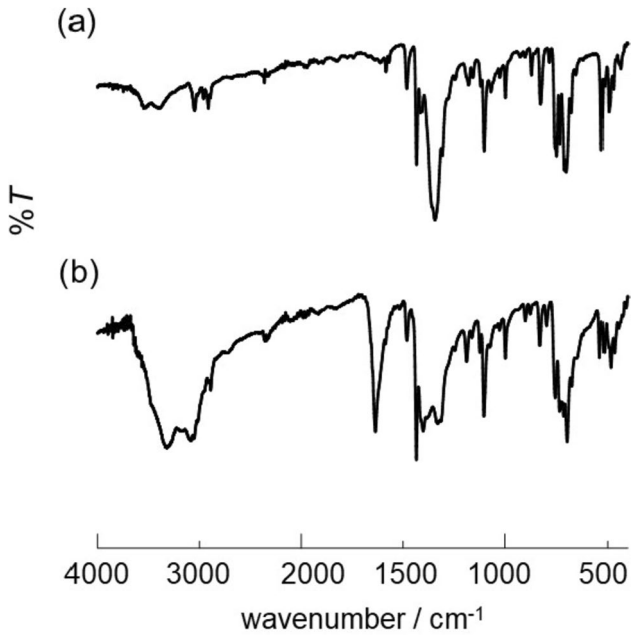

Fig. 1 IR spectra of **a** $[Pt(triphos)_2](NO_3)_2$ and **b** $[Pt(triphos)_2\{Au(tu)\}_2]Cl_2(NO_3)_2$

and the central PPh group. The Pt^{II} center was coordinated by two PPh_2 and PPh groups from the triphos ligands, forming a $[Pt(P_A)_2(P_B)_2]$-type chromophore with a trans configuration, thereby positioning the uncoordinated PPh_2 groups on opposite sides. In addition to cis-trans isomerism around the Pt^{II} center, the coordinated PPh group, which was a stereogenic phosphorous atom, exhibited an R–S configuration, leading to meso(*RS*)-racemic (*RR*/*SS*) isomerism in $[Pt(triphos)_2]^{2+}$. Among the four possible isomers illustrated in Chart 1, $[Pt(triphos)_2](NO_3)_2$ was found to adopt the trans-meso isomer in the crystals. The Pt–PPh_2 (2.3190(9) Å) and Pt–PPh (2.3268(9) Å) bond distances were longer than those in a related $Au^{I}Pt^{II}$ complex with a similar asymmetric triphos coordination mode, $[AuPt(triphos)Cl_3]$ (Pt–PPh_2 = 2.23(1) Å, Pt–PPh = 2.23(1) Å) [24]. Elongation of the Pt–P bonds in $[Pt(triphos)_2](NO_3)_2$ resulted because the trans influence of phosphine groups was larger than that of Cl^- [31, 32], which is why $[Pt(triphos)_2](NO_3)_2$ reached solution equilibrium on the NMR timescale (*vide infra*).

It should be noted that the powder X-ray diffraction pattern of $[Pt(triphos)_2](NO_3)_2$ was consistent with the simulated pattern for the crystal structure, which indicated that only the trans-meso isomer was formed in the bulk sample of $[Pt(triphos)_2](NO_3)_2$ (Fig. 3a). In the packing diagram for $[Pt(triphos)_2](NO_3)_2$, the complex cations formed two intermolecular C–H···π interactions between the phenyl

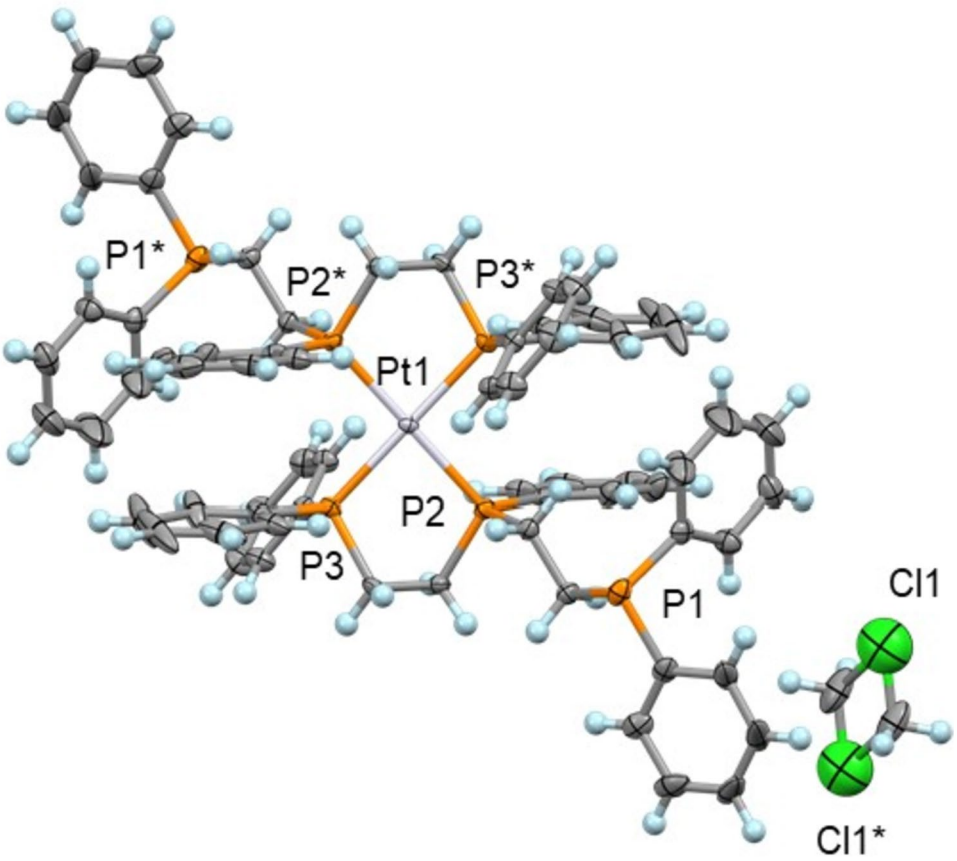

Fig. 2 Perspective view of $[Pt(triphos)_2](NO_3)_2$. The thermal ellipsoids are illustrated at 50% probability. Color code: Pt: white, P: orange, Cl: green, C: gray, H: pale blue. (Color figure online)

Chart 1 Four possible isomers of $[Pt(triphos)_2]^{2+}$; **a** Trans-meso, **b** trans-racemic, **c** cis-meso, and **d** cis-racemic

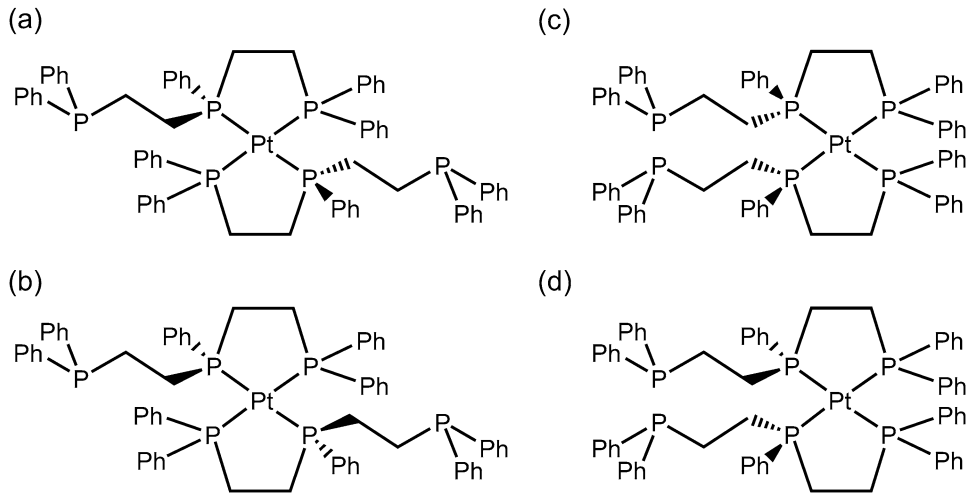

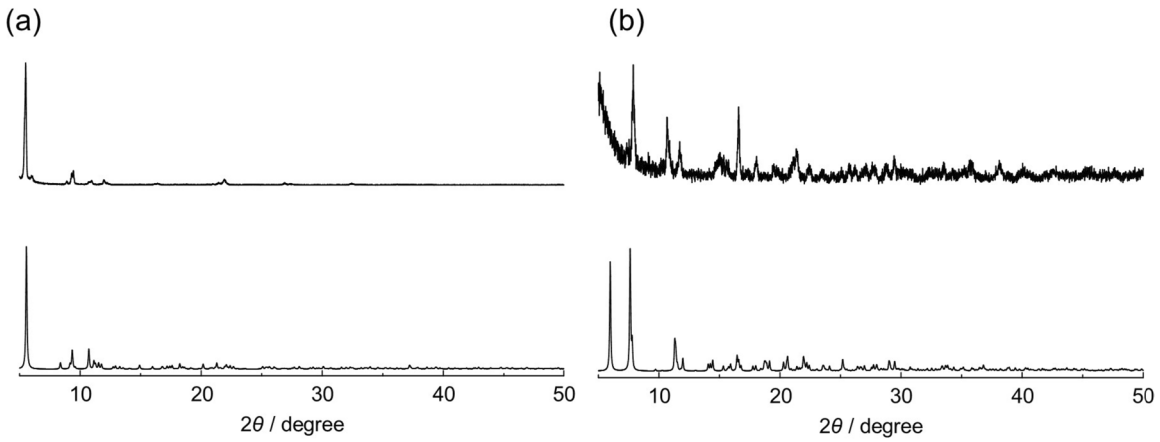

Fig. 3 Observed (top) and simulated (bottom) powder X-ray diffraction patterns for **a** $[Pt(triphos)_2](NO_3)_2$ and **b** $[Pt(triphos)_2\{Au(tu)\}_2]Cl_2(NO_3)_2$

groups of the uncoordinated PPh_2 and coordinated PPh_2 groups (CH···C_g = 2.53 Å and 3.07 Å), creating a 2D sheet supramolecular structure in the crystallographic *ab* plane (Fig. 4a). The 2D structures were stacked along the *c* axis and accommodated the CH_2Cl_2 molecule in the interstitial space (Fig. 4b). We assumed that the adjusted crystal packing to accommodate the CH_2Cl_2 was the key to the selective crystallization of the trans-meso isomer of $[Pt(triphos)_2](NO_3)_2$. Similar solvent-directed crystallization of one of four isomers was observed for a Pt^{II} complex with chlorophosphineamides [16].

Synthesis and structural characterization of $[Pt(triphos)_2\{Au(Tu)\}_2]Cl_2(NO_3)_2$

The $[Pt(triphos)_2](NO_3)_2$ complex contained two unbound PPh_2 groups. Consequently, these groups were anticipated to function as coordination sites for other metal ions, similar to the role of P-donating metalloligands with free phosphine groups, *e.g.*, 1,1'-bis(diphenylphosphino)ferrocene (dppf) [33], (-$PhPC_5H_4FeC_5H_4$-)$_3$ [21], and [Pt(Ar) phenylpyridinates (κ^1-dppm)] [22, 23]. To probe this ability, we examined the reaction of $[Pt(triphos)_2](NO_3)_2$ with two equivalents of $[Au(tu)_2]Cl$, which is a well-known Au^I source [34], in methanol. With addition of excess NaCl to the colorless reaction mixture and subsequent diffusion of diethyl ether vapor, we isolated colorless plate-like crystals of $[Pt(triphos)_2\{Au(tu)\}_2]Cl_2(NO_3)_2$ in satisfactory yield (33%). An X-ray fluorescence analysis revealed that $[Pt(triphos)_2\{Au(tu)\}_2]Cl_2(NO_3)_2$ contained Pt and Au as the metallic elements in a 1:2 ratio, in addition to S, P, and Cl (Fig. S1). The IR spectrum revealed bands due to NO_3^- ions at 1330 cm^{-1}, ν_{P-Ph} (1103, 694 cm^{-1}) and ν_{P-C} (1435, 753 cm^{-1}) bands for the triphos ligands, and ν_{N-H} (3052 cm^{-1}) and $\nu_{C=S}$ (1635 cm^{-1}) bands for the tu ligands (Fig. 1b) [30, 38]. These results supported the formation

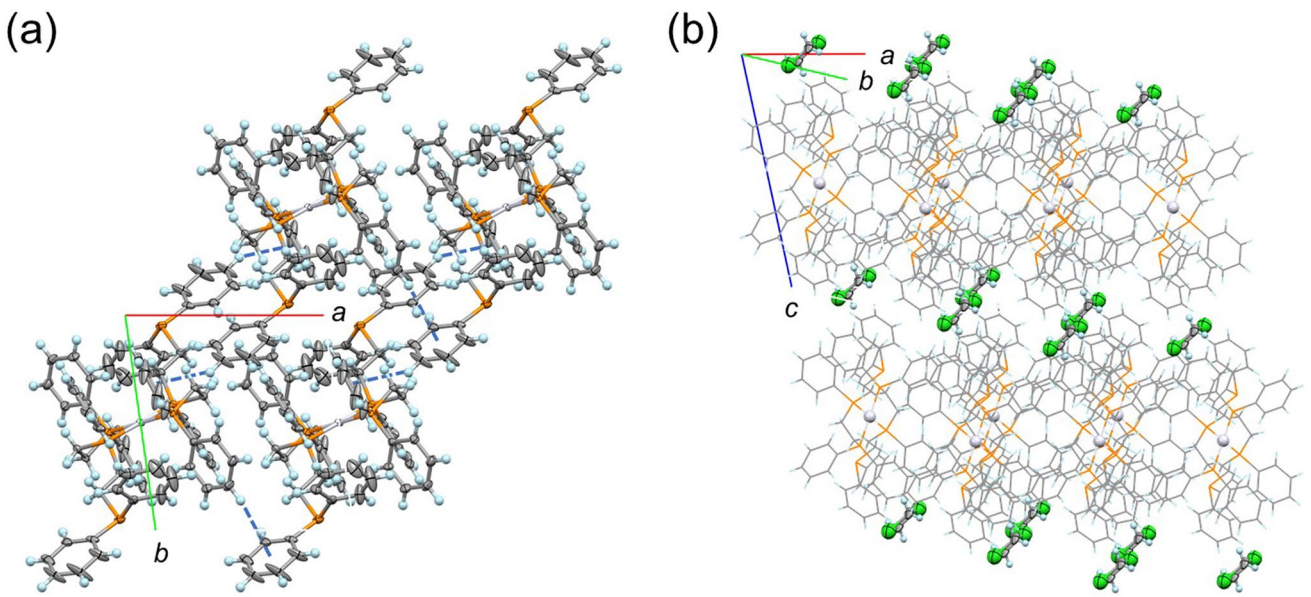

Fig. 4 Perspective views of $[Pt(triphos)_2](NO_3)_2$; **a** 2D sheet supramolecular structure viewed from the *c* axis and **b** packing structure viewed from the *a* axis. The blue dotted lines indicate the CH···π interactions. Color code: Pt: white, P: orange, Cl: green, C: gray, H: pale blue. (Color figure online)

of a 1:2 adduct by the $[Pt(triphos)_2]^{2+}$ and $[Au(tu)]^+$ units. Moreover, the elemental analyses indicated the formula of a double salt, $[Pt(triphos)_2\{Au(tu)\}_2]Cl_2(NO_3)_2{\cdot}5H_2O$. The presence of water molecules was supported by the TG analysis (Fig. S2).

The $[Pt(triphos)_2\{Au(tu)\}_2]Cl_2(NO_3)_2$ crystals showed weak diffraction with the laboratory instrument, so we conducted single-crystal X-ray analyses with the synchrotron faculty at SPring-8. The asymmetric unit contained half of the $Au^I_2Pt^{II}$ complex cation, $[Pt(triphos)_2\{Au(tu)\}_2]^{4+}$ (Fig. 5), which was situated on the crystallographic C_2 axis, and one chloride ion. As found for $[Pt(triphos)_2](NO_3)_{2]}$, two triphos ligands in $[Pt(triphos)_2\{Au(tu)\}_2]^{4+}$ chelated the square-planar Pt^{II} center via bidentate-*P*,*P*' binding. The bond distances around the Pt^{II} center (Pt–PPh_2 = 2.316(3) Å, Pt–PPh = 2.311(3) Å) were similar to those in $[Pt(triphos)_2](NO_3)_2$. However, the Pt^{II} unit had unexpectedly adopted the cis configuration, and the two stereogenic P atoms had the same chirality. That is, the cis-racemic isomer of $[Pt(triphos)_2]^{2+}$ was contained in $[Pt(triphos)_2\{Au(tu)\}_2]Cl_2(NO_3)_2$. The two $\{Au(tu\text{-}S)\}^+$ moieties were bound to the free PPh_2 sites of the $[Pt(triphos)_2]^{2+}$ unit (Au–*P* = 2.265(4) Å, Au–S = 2.314(5) Å, S–Au–*P* = 174.07(15)°) to form a heterometallic trinuclear structure. The powder X-ray diffraction pattern for the bulk sample of $[Pt(triphos)_2\{Au(tu)\}_2]Cl_2(NO_3)_2$ matched the simulated pattern from the crystal data well (Fig. 3b), which confirmed the phase purity of $[Pt(triphos)_2\{Au(tu)\}_2]Cl_2(NO_3)_2$.

In the crystal packing structure, two Cl^- anions were wrapped by the NH_2 groups of the tu ligands and the

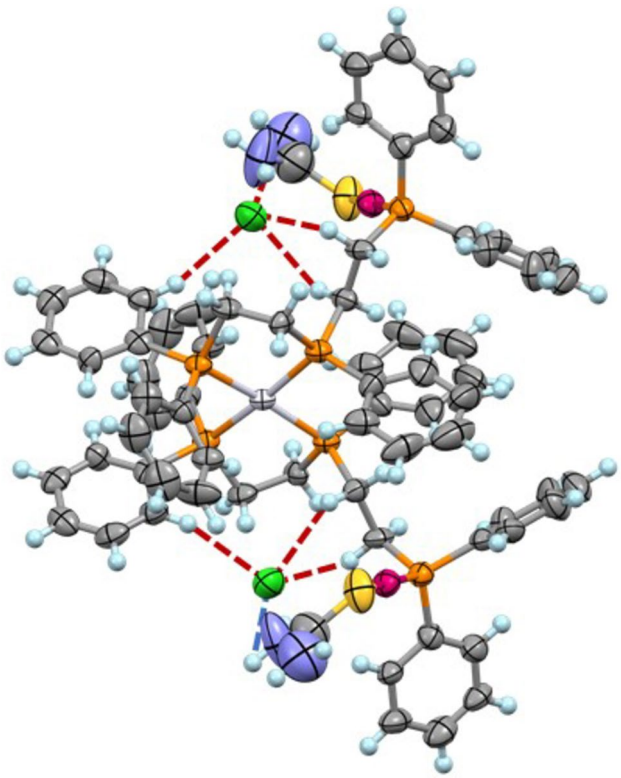

Fig. 5 A perspective view of the complex cation accommodating the Cl^- anion in $[Pt(triphos)_2\{Au(tu)\}_2]Cl_2(NO_3)_2$. The thermal ellipsoids are illustrated at 50% probability. Color code: Pt: white, Au: pink, P: orange, Cl: green, N: blue, C: gray, H: pale blue. The red dotted lines indicate hydrogen bonds. (Color figure online)

ethylene and phenyl groups of the triphos ligands *via* NH···Cl (2.25 Å) and CH···Cl (2.64, 2.62, and 2.94 Å) hydrogen bonds. These interactions resulted in formation of the discrete supramolecule $\{Cl_2@[Pt(triphos)_2\{Au(tu)\}_2]\}^{2+}$ (Fig. 5). We assumed that the interaction between $[Pt(triphos)_2\{Au(tu)\}_2]^{4+}$ and Cl^- led to preferable formation of the cis-racemic isomer of $[Pt(triphos)_2\{Au(tu)\}_2]Cl_2(NO_3)_2$. Moreover, these supramolecules were interconnected by additional CH···Cl hydrogen bonds (2.63 Å) between the phenyl groups and Cl^- anions of adjacent supramolecules, forming a 1D chain structure (Fig. 6a). The 1D chains also interacted with neighboring chains *via* CH···π interactions (CH···C_g = 3.21 and 2.71 Å), culminating in a 3D supramolecular structure with large void spaces (34.2%, 3102.3 $Å^3$ per unit cell) (Fig. 6b). We could not model the nitrate anion and solvated water molecules in the crystal structure because they were severely disordered in the void space.

NMR spectral study

X-ray diffraction experiments revealed that in the solid samples of $[Pt(triphos)_2](NO_3)_2$ and $[Pt(triphos)_2\{Au(tu)\}_2]Cl_2(NO_3)_2$, the $[Pt(triphos)_2]^{2+}$ units selectively formed the trans-meso- and cis-racemic isomers, respectively. To investigate the molecular structure in solution, we performed NMR spectroscopic measurements of these compounds in methanol-d_4. The ^{1}H NMR spectra were complicated (Fig. S3); therefore, our analysis was primarily focused on the ^{31}P NMR spectra. The ^{31}P NMR spectrum of $[Pt(triphos)_2](NO_3)_2$ determined in methanol-d_4 at 25 °C exhibited two singlet signals with platinum satellites at δ 46.28 (signal A) and 19.02 ppm (signal B) with an integration intensity ratio of 1:2 (Fig. 7a). The coupling constant J_{P-Pt} of signal A (1087 Hz) was approximately twice that of signal B (622.6 Hz). These spectral features were inconsistent with the C_s symmetric mononuclear structure observed in the single-crystal X-ray study, which should display two singlets with similar J_{P-Pt} values alongside one singlet without platinum satellites. We tentatively assigned the ^{31}P signals A and B to the central PPh and terminal PPh_2 groups of triphos ligands, respectively, and we presumed that the coordinated and uncoordinated PPh_2 groups rapidly exchanged on the NMR timescale. To verify this dynamic behavior, we measured the variable-temperature (VT) NMR spectra at temperatures from 25 °C to − 80 °C. Upon cooling, signals A and B became broader at -40 °C and disappeared at lower temperatures. At − 80 °C, a new singlet without platinum satellites appeared at − 15.23 ppm (signal C), which indicated uncoordinated PPh_2 groups, as typically reported in the literature [36]. Additionally, complex, broad signals appeared between δ 15–50 ppm. We hypothesized that all or some of the four possible stereoisomers of $[Pt(triphos)_2]^{2+}$ (cis-meso, cis-racemic, trans-meso, and trans-racemic) were in equilibrium in solution, and an average structure was observed at 25 °C. Exchange among the isomers required Pt–P bond cleavage. The Pt–P bonds were elongated, which was attributed to the substantial trans influence of the phosphines, may have facilitate bond cleavage within the system.

The ^{31}P NMR spectrum of $[Pt(triphos)_2\{Au(tu)\}_2]Cl_2(NO_3)_2$ determined in methanol-d_4 at 25 °C showed two singlets with platinum satellites at 92.21 (J_{P-Pt} = 1342 Hz) and 43.37 (J_{P-Pt} = 1211 Hz) ppm ascribed to the Pt-PPh_2 and Pt-PPh groups, respectively. In addition,

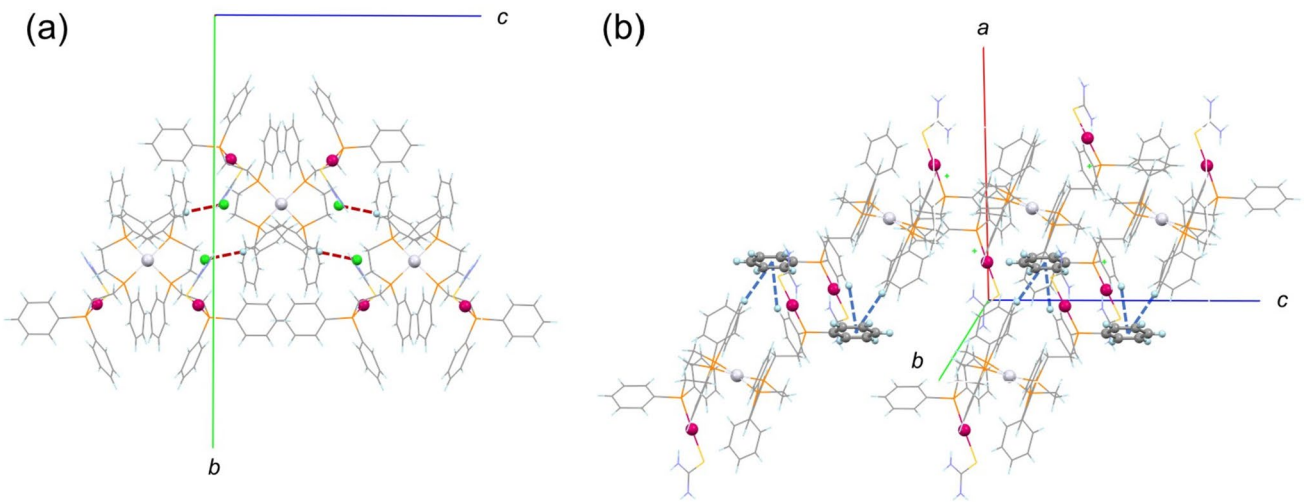

Fig. 6 Perspective views of $[Pt(triphos)_2\{Au(tu)\}_2]Cl_2(NO_3)_2$. **a** The 2D chain structure viewed from the *b* axis. **b** The packing structure viewed from the *a* axis. The red and blue dotted lines indicate the hydrogen bonds and CH···π interactions, respectively. Color code: Pt: white, Au: pink, P: orange, Cl: green, N: blue, C: gray, H: pale blue. (Color figure online)

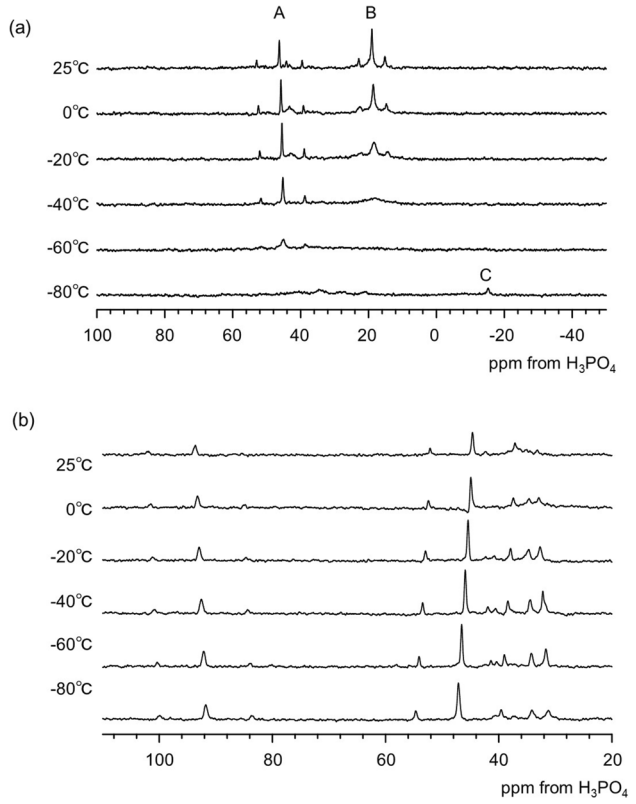

Fig. 7 VT ^{31}P NMR spectra of **a** $[Pt(triphos)_2](NO_3)_2$ and **b** $[Pt(triphos)_2\{Au(tu)\}_2]Cl_2(NO_3)_2$ determined in methanol-d_4

the spectrum showed two singlets without platinum satellites at 34.6 and 33.2 ppm due to the Au-PPh_2 group (Fig. 7b). The overall spectrum was consistent with the C_2 symmetric trinuclear $Au^I_2Pt^{II}$ structure observed in the single-crystal X-ray analysis, except for the appearance of two signals due to the Au-PPh_2 groups. The signal splitting presumably resulted from partial exchange of the tu ligands with the solvent in solution. Note that the VT NMR spectra of $[Pt(triphos)_2\{Au(tu)\}_2]Cl_2(NO_3)_2$ from 25 to − 80 °C showed no drastic spectral changes, unlike that of $[Pt(triphos)_2](NO_3)_2$. Au-P bond formation may have suppressed Pt-P bond exchange, which maintained the cis-racemic isomer of $[Pt(triphos)_2\{Au(tu)\}_2]Cl_2(NO_3)_2$ even in solution.

Photophysical properties

The absorption spectra of the $[Pt(triphos)_2](NO_3)_2$ and $[Pt(triphos)_2\{Au(tu)\}_2]Cl_2(NO_3)_2$ complexes in methanol exhibited π-π* transition bands below 270 nm due to the Ph groups of the triphos ligands and a ^{1}MLCT transition from Pt^{II} to the phosphine groups at approximately 320 nm (Fig. S4) [37]. In addition, $[Pt(triphos)_2](NO_3)_2$ showed a weak visible band at approximately 400 nm due to the ^{3}MLCT transition.

The solid samples of $[Pt(triphos)_2](NO_3)_2$ and $[Pt(triphos)_2\{Au(tu)\}_2]Cl_2(NO_3)_2$ showed emission at 77 K. The excitation and emission spectra are illustrated in Fig. 8. The excitation spectra of the two complexes showed π–π* bands at approximately 280 nm and ^{1}MLCT bands at approximately 330 nm. The similar excitation spectra indicated that cis-trans isomerism around the Pt^{II} center and the presence/absence of the $\{Au(tu)\}^+$ moieties did not affect the absorption spectrum. However, the emission band for $[Pt(triphos)_2\{Au(tu)\}_2]Cl_2(NO_3)_2$ (λ_{em} = 474 nm) occurred at a longer wavelength than that of $[Pt(triphos)_2](NO_3)_2$ (λ_{em} = 438 nm). Moreover, the emission band for $[Pt(triphos)_2\{Au(tu)\}_2]Cl_2(NO_3)_2$ revealed a structured pattern with a separation of ca. 1600 cm^{-1}. This value

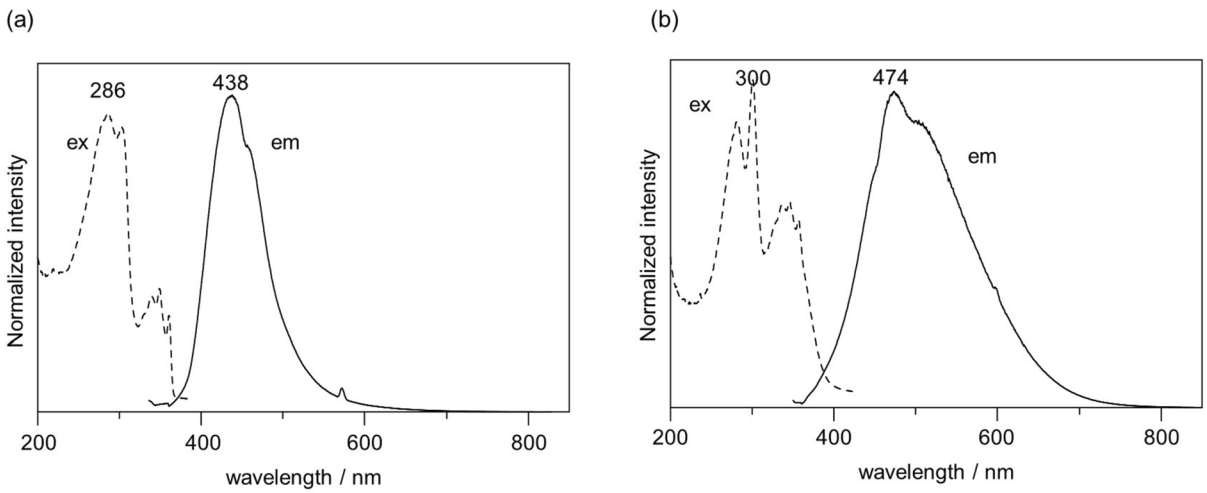

Fig. 8 Excitation (ex) and emission (em) spectra of **a** $[Pt(triphos)_2](NO_3)_2$ and **b** $[Pt(triphos)_2\{Au(tu)\}_2]Cl_2(NO_3)_2$ in the solid-state at 77 K

was similar to the C=S stretching energy (1635 cm^{-1}) of the tu ligand in $[Pt(triphos)_2\{Au(tu)\}_2]Cl_2(NO_3)_2$, which was observed in the IR spectra (*vide supra*). Therefore, we propose that the emission of $[Pt(triphos)_2](NO_3)_2$ involved charge transfer from Pt^{II} to a phosphine (^{3}MLCT) of the $[PtP_4]$ moiety, while the emission of $[Pt(triphos)_2\{Au(tu)\}_2]Cl_2(NO_3)_2$ was ascribed to charge transfer from S to P (^{3}LLCT) or S to Au (^{3}LMCT) [38]. The large Stokes shift for $[Pt(triphos)_2\{Au(tu)\}_2]Cl_2(NO_3)_2$ was explained by intramolecular energy transfer from the $[PtP_4]$ to [AuPS] moieties and structural distortion of the Au^I ion in the triplet state. The quantum yields (Φ) of the two complexes were 6.9% for $[Pt(triphos)_2](NO_3)_2$ and 16% for $[Pt(triphos)_2\{Au(tu)\}_2]Cl_2(NO_3)_2$. Multiple H bonds between the complex cationa and Cl^- may have reduced the molecular vibrations, which may have contributed to the strong photoluminescence from the $Au^I_2Pt^{II}$ complex $[Pt(triphos)_2\{Au(tu)\}_2]Cl_2(NO_3)_2$.

Concluding remarks

We crystallized and elucidated the structure of $[Pt(triphos)_2](NO_3)_2$, in which two triphos ligands were chelated to the square-planar Pt^{II} center with two of three P atoms. We also showed that the $[Pt(triphos)_2]^{2+}$ complex acted as P-donating metalloligands for Au^I ions by utilizing the two remaining P atoms. This was evidenced by formation of the trinuclear $Au^I_2Pt^{II}$ complex $[Pt(triphos)_2\{Au(tu)\}_2]Cl_2(NO_3)_2$, which was synthesized by reacting $[Pt(triphos)_2](NO_3)_2$ with $[Au(tu)_2]Cl$. Notably, we observed a structural transformation within the $[Pt(triphos)_2]^{2+}$ unit; the trans-meso isomer present in $[Pt(triphos)_2](NO_3)_2$ underwent conversion to the cis-racemic isomer in $[Pt(triphos)_2\{Au(tu)\}_2]Cl_2(NO_3)_2$. An NMR spectral analysis suggested that this unique trans-to-cis isomerization of the Pt^{II} center was triggered by the reaction with Au^I and occurred through rapid equilibrium among the possible isomers in solution. The complexes $[Pt(triphos)_2](NO_3)_2$ and $[Pt(triphos)_2\{Au(tu)\}_2]Cl_2(NO_3)_2$ showed photoluminescence at 77 K. The higher luminescence quantum yield for $[Pt(triphos)_2\{Au(tu)\}_2]Cl_2(NO_3)_2$ relative to that for $[Pt(triphos)_2](NO_3)_2$ was tentatively explained by the presence of multiple hydrogen bonds with Cl^-, which may have suppressed vibrational quenching of the photoluminescence in $[Pt(triphos)_2\{Au(tu)\}_2]Cl_2(NO_3)_2$. Finally, the present study demonstrated that square-planar Pt^{II} species with two triphosphine ligands can serve as P-donating metalloligands with dynamic geometric isomerism for the future design and creation of switchable luminescent materials.

Supplementary Information The online version contains supplementary material available at https://doi.org/10.1007/s10847-024-01228-2.

Acknowledgements This work was supported by JSPS KAKENHI (Grant No. 19K05496). The synchrotron radiation experiments were performed at the BL02B1 beamline of SPring-8 with the approval of the Japan Synchrotron Radiation Research Institute (JASRI) (Proposal Nos. 2022A1573 and 2022B1659). This work is the result of using research equipment shared in MEXT Project for promoting public utilization of advanced research infrastructure (Program for supporting construction of core facilities) Grant Number JPMXS0441200023.

Author contributions KN and HS prepared compounds; KN and TB conducted compound characterization; TB and NY wrote the draft; NY edited the manuscript, and conceived the project. All authors have given approval to the final version of the manuscript.

Funding Open Access funding provided by Osaka University.

Data availability Crystallographic data (including structure factors) for the structures reported in this paper have been deposited with the Cambridge Crystallographic Data Centre. CCDC numbers: 2327654 for $[Pt(triphos)_2](NO_3)_2$ and 2327655 for $[Pt(triphos)_2\{Au(tu)\}_2]Cl_2(NO_3)_2$. Copies of the data can be obtained free of charge on application to CCDC, https://www.ccdc.cam.ac.uk/structures/.

Declarations

Competing interests The authors declare no competing interests.

Supporting information The fluorescence X-ray spectra (Fig. S1), TG profiles (Fig. S2), ^{1}H NMR spectra (Fig. S3), and absorption spectra (Fig. S4) are included in the supplementary material in PDF format. The crystallographic data (including the structure factors) for the structures reported in this paper have been deposited with the Cambridge Crystallographic Data Centre. CCDC numbers: 2327654 for $[Pt(triphos)_2](NO_3)_2$ and 2327655 for $[Pt(triphos)_2\{Au(tu)\}_2]Cl_2(NO_3)_2$. Copies of the data can be obtained free of charge on application to the CCDC, https://www.ccdc.cam.ac.uk/structures/.

Open Access This article is licensed under a Creative Commons Attribution 4.0 International License, which permits use, sharing, adaptation, distribution and reproduction in any medium or format, as long as you give appropriate credit to the original author(s) and the source, provide a link to the Creative Commons licence, and indicate if changes were made. The images or other third party material in this article are included in the article's Creative Commons licence, unless indicated otherwise in a credit line to the material. If material is not included in the article's Creative Commons licence and your intended use is not permitted by statutory regulation or exceeds the permitted use, you will need to obtain permission directly from the copyright holder. To view a copy of this licence, visit http://creativecommons.org/licenses/by/4.0/.

References

1. Gispert, J.R.: Coordination Chemistry. Wiley-VCH Verlag GmbH & Co. KGaA, Weinheim, Germany (2008)
2. Kishimoto, T., Yoshikawa, Y., Yoshikawa, K., Komeda, S.: Different effects of Cisplatin and Transplatin on the higher-order structure of DNA and gene expression. Int. J. Mol. Sci. **21**, 34 (2020). https://doi.org/10.3390%2Fijms21010034
3. Patterson, H.H., Tewksbury, J.C., Martin, M., Krogh-Jespersen, M.-B., Lomenzo, J.A., Hooper, H.O., Viswanath, A.K.: Luminescence, absorption, MCD, and NQR Study of the Cis and Trans Isomers of Dichlorodiammineplatinum(II). Inorg. Chem. **20**, 2297–2301 (1981). https://doi.org/10.1021/ic50221a071
4. Konno, T., Yoshinari, N., Taguchi, M., Igashira-Kamiyama, A.: Drastic change in Dimensional structures of d-Penicillaminato $(Au^I_2Pt^{II}_2Zn^{II})_n$ coordination polymers by Moderate Change in

Solution pH. Chem. Lett. **38**, 526–527 (2009). https://doi.org/10.1021/ic50221a071
5. Yoshinari, N., Hashimoto, Y., Igashira-Kamiyama, A., Konno, T.: Synthesis, characterization, and Crystal Structures of Cis and trans isomers of a platinate(II) complex with d-Penicillaminate. Bull. Chem. Soc. Jpn. **84**, 623–625 (2011). https://doi.org/10.1246/bcsj.20110036
6. Geist, F., Jackel, A., Winter, R.F.: Synthesis, Ligand Based Dual Fluorescence and Phosphorescence Emission from BODIPY Platinum Complexes and its application to Ratiometric Singlet Oxygen Detection. Inorg. Chem. **54**, 10946–10957 (2015). https://doi.org/10.1021/acs.inorgchem.5b01969
7. Mastin, S.H., Haake, P.: Synthesis of trans-platinum(II) complexes by photochemical isomerization. J. Chem. Soc. D. **6**, 202 (1970). https://doi.org/10.1039/C29700000202
8. Ube, H., Yasuda, Y., Sato, H., Shionoya, M.: Metal-centred azaphosphatriptycene gear with a photo- and thermally driven mechanical switching function based on coordination isomerism. Nat. Commun. **8**, 14296 (2017). https://doi.org/10.1038/ncomms14296
9. Pascui, A.E., Rees, K.V., Zant, D.W., Broere, D.L.J., Siegler, M.A., Vlugt, J.I.V.D.: Macrocyclic platinum(II) complexes with a bifunctional Diphosphine Ligand. Eur. J. Inorg. Chem. **34**, 5578–5714 (2015). https://doi.org/10.1002/ejic.201501055
10. Melník, M., Mikuš, P.: Organodiphosphines in Pt{η^2-P(X)$_n$P}Cl$_2$ (n = 9–15, 17, 18) derivatives – structural aspects. Rev. Inorg. Chem. **41**, 41–48 (2021). https://doi.org/10.1515/revic-2020-0010
11. Owens, S.B. Jr., Smith, D.C. Jr., Lake, C.H., Gray, F.M.: Synthesis, characterization, and cis-trans isomerization studies of cis-[PdCl$_2${Ph$_2$P(CH$_2$CH$_2$O)$_3$CH$_2$CH$_2$PPh$_2$-P,P'}] and trans-[PtCl$_2${Ph$_2$P(CH$_2$CH$_2$O)$_3$CH$_2$CH$_2$PPh$_2$-P,P'}] Metallacrown Ethers. Eur. J. Inorg. Chem. **30**, 4710–4718 (2008). https://doi.org/10.1515/revic-2020-0010
12. Romeo, R., Minniti, C., Trozzi, M.: Uncatalyzed Cis-trans isomerization and methanol solvolysis of Arylbromobis(triethylphosphine)platinum(II) complexes. A different role for Steric Hindrance in Dissociative and associative mechanisms. Inorg. Chem. **15**, 1134–1138 (1976). https://doi.org/10.1515/revic-2020-0010
13. Zhang, S., Pattacini, R., Braunstein, P., Cola, L.D., Plummer, E., Mauro, M., Doulaouen, C., Daniel, C.: Synthesis, structure, and Optical properties of Pt(II) and pd(II) complexes with oxazolyl- and pyridyl-functionalized DPPM-Type ligands: A combined experimental and theoretical study. Inorg. Chem. **53**, 12739–12756 (2014). https://doi.org/10.1021/ic501566u
14. Zhang, S., Pattacini, R., Braunstein, P.: Unexpected Metal-Induced isomerisms and Phosphoryl migrations in Pt(II) and pd(II) complexes of the functional phosphine 2-(Bis(diphenylphosphino) methyl)-oxazoline. Inorg. Chem. **50**, 3511–3522 (2011). https://doi.org/10.1021/ic1024422
15. Redwine, K.D., Wilson, W.L., Moses, D.G., Catalano, V.J., Nelson, J.H.: Cooperative Diastereoselectivity of Palladium- and platinum-promoted intramolecular [4 + 2] diels – alder cycloaddition reactions of 3,4-Dimethyl-1-phenylphosphole. Inorg. Chem. **39**, 3392–3402 (2000). https://doi.org/10.1021/ic990885j
16. Lungu, D., Daniliuc, C., Jones, P.G., Nyulászi, L., Benkõ, Z., Bartsch, R., Mont, W.-W.D.: Exceptional Coordination Mode of Unsaturated PNP ligands (Me$_3$Si)$_2$C=PN(R)PPh$_2$ with palladium and platinum dichlorides: Insertion of Phosphaalkene Phosphorus atoms into metal–chlorine bonds. Eur. J. Inorg. Chem. **20**, 2901–2905 (2009). https://doi.org/10.1002/ejic.200900236
17. Deeming, A.J., Cockerton, B.R., Doherty, S.: Substitution of chloride in [PtCl$_2$(PEt$_3$)$_2$] by the chiral anionic ligand [Mo(CO)$_5$(PPhH)]$^-$ to give mixed platinum-molybdenum compounds and a ^{31}P{^{1}H} NMR analysis of their fluxionality. X-ray crystal structure of [PtCl(PEt$_3$)$_2$(μ-PPhH){Mo(CO)$_5$}] and trans-[Pt(PEt$_3$)$_2$(μ-PPH)$_2${Mo(CO)$_5$}$_2$]. Polyhedron. **16**, 1945–1956 (1997). https://doi.org/10.1016/S0277-5387(96)00403-2
18. Barkley, J., Higgins, S.J., McCart, M.K.: Complexes of 2,3-bis(diphenylphosphino)propene with Pt^{II}, Pd^{II} and Ru^{II}: Synthesis, characterisation and rearrangements to complexes of cis-1,2-bis(diphenylphosphino)propene. J. Chem. Soc. Dalton Trans. **16**, 1787–1792 (1998). https://doi.org/10.1016/S0277-5387(96)00403-2
19. García-Seijo, M.I., Castiñeiras, A., Mahieu, B., Jánosi, L., Berente, Z., Kollár, L., García-Fernández, M.E.: Crystal structure and reactivity of mononuclear cationic palladium(II) and platinum(II) triphos complexes with phenyltin(IV) anions. The formation of polynuclear platinum–triphos ionic and covalent complexes. Polyhedron. **20**, 855–868 (2001). https://doi.org/10.1016/S0277-5387(96)00403-2
20. Balch, A.L., Catalano, V.J.: Formation of luminescent, metal-metal bonded, 3:5 complexes using palladium(II) or platinum(II) and iridium(I) through chelate ring openings. Inorg. Chem. **31**, 2569–2575 (1992). https://doi.org/10.1021/ic00038a048
21. Mizuta, T., Aotani, T., Imamura, Y., Kubo, K., Miyoshi, K.: Structure and Properties of the Macrocyclic Tridentate Ferrocenylphosphine Ligand (-PhPC$_5$H$_4$FeC$_5$H$_4$-)$_3$. Organometallics. **27**, 2457–2463 (2008). https://doi.org/10.1021/om800057w
22. Dolatyari, V., Shahsavari, H.R., Fereidoonnezhad, M., Farhadi, F., Akhlaghi, S., Latouche, C., Latouche, C., Sakamaki, Y., Beyzavi, H.: Luminescent heterobimetallic PtII–AuI complexes bearing N-Heterocyclic carbenes (NHCs) as potent Anticancer agents. Eur. J. Inorg. Chem. **10**, 1360–1373 (2019). https://doi.org/10.1021/acs.inorgchem.3c01504
23. Shahsavari, H.R., Giménez, N., Lalinde, E., Moreno, M.T., Fereidoonnezhad, M., Aghakhanpour, R.B., Khatami, M., Kalantari, F., Jamshidi, Z., Mohammadpour, M.: Luminescent heterobimetallic Pt^{II}–Au^{I} complexes bearing N-Heterocyclic carbenes (NHCs) as potent Anticancer agents. Inorg. Chem. **62**, 13241–13252 (2019). https://doi.org/10.1002/ejic.201801297
24. Sevillano, P., Habtemariam, A., Parsons, S., Castiñeiras, A., García, M.E., Sadler, P.J.: Gold(I)-induced chelate ring-opening of palladium(II) and platinum(II) triphos complexes. J. Chem. Soc. Dalton Trans. **16**, 2861–2870 (1999). https://doi.org/10.1002/ejic.201801297
25. Piro, O.E., Castellano, E.E., Piatti, R.C.V., Bolzán, A.E., Arvia, A.J.: Two thiourea-containing gold(I) complexes. Acta Cryst. **C58**, m252–m255 (2002). https://doi.org/10.1002/ejic.201801297
26. Macrae, C.F., Sovago, I., Cottrell, S.J., Galek, P.T.A., McCabe, P., Pidcock, E., Platings, M., Shields, G.P., Stevens, J.S., Towler, M., Wood, P.A.: Mercury 4.0: From visualization to analysis, design and prediction. J. Appl. Cryst. **53**, 226–235 (2020). https://doi.org/10.1107/S1600576719014092
27. Sheldrick, G.M.: A short history of SHELX. Acta Cryst. **A64**, 112–122 (2008). https://doi.org/10.1107/S1600576719014092
28. Sheldrick, G.M.: Crystal structure refinement with SHELXL. Acta Cryst. C. **71**, 3–8 (2015). https://doi.org/10.1107/S2053229614024218
29. Dolomanov, O.V., Bourhis, L.J., Gildea, R.J., Howard, J.A.K., Puschmann, H.J.: OLEX2: A complete structure solution, refinement and analysis program. J. Appl. Cryst. **42**, 339–341 (2009). https://doi.org/10.1107/S0021889808042726
30. Socrates, G.: Infrared Characteristic Group Frequencies, 3rd edn. Wiley, Chichester, UK (2001)
31. Kapoor, P., Kukushkin, V.Y., Lövqvist, K., Oskarsson, Å.: Trans influence in platinum(II) complexes. Phenylation of pt(II) dialkylsulfide complexes by BPh$_4^-$ and SnPh$_3$H. Crystal structures of two polymorphs of trans-chlorobis(dimethylsulfide)(phenyl) platinum(II). J. Organomet. Chem. **517**, 71–79 (1996). https://doi.org/10.1016/0022-328X(95)06103-4

32. Chval, Z., Sip, M., Burda, J.V.: The trans effect in square-planar platinum(II) complexes—A density functional study. J. Comput. Chem. **29**, 2370–2381 (2008). https://doi.org/10.1002/jcc.20980
33. Hrubý, J., Dvořák, D., Squillantini, L., Mannini, M., Slageren, J.V., Herchel, R., Nemec, I., Neugebauer, P.: Co(II)-Based single-ion magnets with 1,1'-ferrocenediyl-bis(diphenylphosphine) metalloligands. Dalton Trans. **49**, 11697–11707 (2020). https://doi.org/10.1039/D0DT01512A
34. Isab, A.A., Fettouhi, M., Ahmad, S., Ouahab, L.: Mixed ligand gold(I) complexes of phosphines and thiourea and X-ray structure of (thiourea-κS)(tricyclohexylphosphine)gold(I)chloride. Polyhedron. **22**, 1349–1354 (2003). https://doi.org/10.1016/S0277-5387(03)00129-3
35. Jensen, K.A., Nielsen, P.H.: Infrared Spectra of thioamides and Selenoamides. Acta Chem. Scand. **20**, 597–629 (1966). https://doi.org/10.3891/acta.chem.scand.20-0597
36. Mason, L.J., Moore, A.J., Carr, A., Helm, M.L.: Lithium bis(2-phenylphosphidoethyl)phenyl-phosphine: A reactive phosphorus intermediate. Heteroat. Chem. **18**, 675–678 (2007). https://doi.org/10.1002/hc.20351
37. Solar, J.M., Ozkan, M.A., Isci, H., Mason, W.R.: Electronic absorption and magnetic circular dichroism spectra of some planar platinum(II), palladium(II), and nickel(II) complexes with phosphorus-donor ligands. Inorg. Chem. **23**, 758–764 (1984). https://doi.org/10.1021/ic00174a024
38. Hashimoto, Y., Yoshinari, N., Naruse, D., Nozaki, K., Konno, T.: Synthesis, structures, and Luminescence properties of Interconvertible $Au^{I}_{2}Zn^{II}$ and $Au^{I}_{3}Zn^{II}$ complexes with mixed bis(diphenylphosphino)methane and d-Penicillaminate. Inorg. Chem. **52**, 14368–14375 (2013). https://doi.org/10.1021/ic4024629

Publisher's Note Springer Nature remains neutral with regard to jurisdictional claims in published maps and institutional affiliations.